

Learning Dynamic Graph Embeddings with Neural Controlled Differential Equations

Tiexin Qin

City University of Hong Kong

TIEXINQIN2-C@MY.CITYU.EDU.HK

Benjamin Walker

University of Oxford

BENJAMIN.WALKER2@BALLIOL.OX.AC.UK

Terry Lyons

University of Oxford

TLYONS@MATHS.OX.AC.UK

Hong Yan

City University of Hong Kong

ITYAN@CITYU.EDU.HK

Haoliang Li

City University of Hong Kong

HAOLIANG.LI1991@GMAIL.COM

Abstract

This paper focuses on representation learning for dynamic graphs with temporal interactions. A fundamental issue is that both the graph structure and the nodes own their own dynamics, and their blending induces intractable complexity in the temporal evolution over graphs. Drawing inspiration from the recent process of physical dynamic models in deep neural networks, we propose *Graph Neural Controlled Differential Equation* (GN-CDE) model, a generic differential model for dynamic graphs that characterise the continuously dynamic evolution of node embedding trajectories with a neural network parameterised vector field and the derivatives of interactions *w.r.t.* time. Our framework exhibits several desirable characteristics, including the ability to express dynamics on evolving graphs without integration by segments, the capability to calibrate trajectories with subsequent data, and robustness to missing observations. Empirical evaluation on a range of dynamic graph representation learning tasks demonstrates the superiority of our proposed approach compared to the baselines.

Keywords: Dynamic graph, embedding learning, controlled differential equation

1. Introduction

Graph representation learning analyzes complex structured data by representing node attributes and relationships in a low-dimensional vector space. In recent years, it has attracted increasing attention owing to the prevalent presence of graph-structured data. The use of deep neural networks, particularly graph neural networks (GNNs), has further facilitated the ability of graph representation learning to represent nodes. For example, GNNs have been used to study social media (Fan et al. 2019; Sankar et al. 2021), protein interactions (Gainza et al. 2020), traffic flow forecasting (Lan et al. 2022), and neuroscience (Bessadok et al. 2022).

Many applications of graph representation learning involve temporal interactions, yet most existing methods do not consider such dynamics. As Xu et al. (2020) pointed out, ignoring the temporal evolution in dynamic graphs can result in suboptimal performance. In certain scenarios, the dynamic structure holds key insights into the system. For example, when using a pandemic model to predict the spread of infection, the evolution of social relationships due to human events

(e.g., immigration, travel, education) must be taken into account (Zhong 2021). In another example, malignant cells within tumors secrete proteins that influence neighboring stromal cells and create an environment conducive to their growth and metastasis (Podhajcer et al. 2008). For more examples, see Kazemi et al. (2020).

In this article, we focus upon the realm of representation learning for dynamic graphs, where explicitly modeling both the time- and node-dependent interactions is generally required to better represent temporal evolution and the dynamic nature of the data. Despite the importance, it can be rather challenging to capture both of these dynamics effectively, mainly when the changes are continuous-time and nonlinear. While learning representations on dynamic graphs is a relatively new field, prior works are limited to discrete-time dynamic graphs, which are represented as a sequence of snapshots of the graph (Goyal et al. 2018; Kumar et al. 2019; Pareja et al. 2020; Chen et al. 2021). Recently, Ordinary Differential Equations (ODEs) have been incorporated into graph neural networks for continuous-time dynamic scenarios (Zang and Wang 2020; Yan et al. 2021; Choi et al. 2022). Nevertheless, these approaches still rely on a static graph structure or segments of static graphs for dynamic inference.

To address these limitations, we propose a novel and unified framework for dynamic graph representation learning that can handle both *the structural dynamics* and *the intrinsic dynamics of nodes* simultaneously, wherein the node embeddings are considered to undergo a dynamic evolution over time, in a manner similar to the concept of Neural Controlled Differential Equations (Neural CDEs) (Kidger et al. 2020) built for time series tasks. Neural CDEs are a powerful concept that has desired calibration ability with subsequent data, robustness to missing values and a memory-efficient property based on adjoint-based backpropagation. We extend this concept to dynamic graphs, which we refer to as the Graph Neural Controlled Differential Equation (GN-CDE) model. The main difference is that GN-CDE creates a continuous path for temporal interactions among two nodes, allowing both structural dynamics and intrinsic dynamics to be naturally incorporated into the integration process. This makes GN-CDE not simply an extension of Neural CDEs, as it can handle the causal effects inherent in dynamic graph structures while the original Neural CDEs cannot. Excitingly, the capability of adjusting the predicted trajectories with incoming even partially observed data and training via adjoint backpropagation from Neural CDEs still hold for our model, making it a promising method for practical usage. It is worth noting that, GN-CDE is a flexible framework that we can leverage to tackle node attribute prediction, dynamic node classification and temporal link prediction tasks with minor modifications. Besides, it can easily be extended to more complex graph structures (such as directed graphs and knowledge graphs). To demonstrate the superiority of our method, we further experimentally evaluate it on node attribute prediction tasks with the underlying graph structure evolving and our method can achieve favorable results across different setups. The contributions of this work are summarized below.

- We propose a generic model GN-CDE which expresses the graph structural dynamics via creating graph paths into our controlled differential equation for dynamic graphs, allowing modeling the continuously evolving process of node embeddings.
- Two alternative approaches are presented, and their theoretical properties are analyzed for comparative purposes.
- We further propose an approximation for the integration process that not only results in a more efficient implementation, but also allows for more flexibility in message passing between graphs.

- Experimental results verify that our proposed method can achieve better results than other methods across different graph tasks.

1.1. Related Works

Graph Embedding Learning. Early works for graph representation learning include graph factorization approaches (Belkin and Niyogi 2001; Ahmed et al. 2013) and random walk-based methods (Perozzi et al. 2014; Tang et al. 2015). With the success of deep learning, Graph Neural Networks which learn node representations by aggregating neighborhood features at each layer, achieve outstanding performance in various tasks (Welling and Kipf 2016; Hamilton et al. 2017; Veličković et al. 2017). However, all the above methods are only limited to node representation learning with a static graph structure.

In the real world, graphs are inherently dynamic rather than static. For example, the interactions of users can change from time to time for e-commerce and social platforms. Existing works for tackling such dynamics can be roughly categorized into three categories. The first type focuses on capturing temporal information along with local structure so as to enhance the expressive ability of the model (Yan et al. 2018; Pareja et al. 2020; Ma et al. 2020; Lan et al. 2022). Specifically, it can be achieved via learning new parameters for each snapshot and maintaining the shareable temporal information. The second type investigates the efficient update schemes when the graph structure changes (Kumar et al. 2019; Rossi et al. 2020; Chen et al. 2021), wherein the interaction events are classified in a fine-grained manner, and the nodes only update when affected by some events. Very recently, differential equations have been incorporated with graph neural networks for dynamic graphs (Zang and Wang 2020; Yan et al. 2021; Choi et al. 2022). These methods are capable of processing irregularly sampled observations and inferring the continuous dynamics of nodes. It is this last one that is of most interest to us here. Unlike these methods limited to a fixed graph structure only, we propose a graph neural controlled differential equations model to incorporate the graph structural dynamics when integrating over graphs. As a result, the requirement for a static graph can be eliminated naturally.

Neural Differential Equations. Neural differential equations are an attractive option for modeling temporal dynamics on hidden representations via using a neural network to parameterize the vector field (Chen et al. 2018; Kidger et al. 2020). The majority of existing work aims to utilize such integration procedure to stimulate neural networks with infinite depth, thus the representation ability can be strengthened. For example, Neural ODEs are analog to a continuous version of ResNet (Chen et al. 2018). Neural CDEs correspond to Recurrent Neural Network (Kidger et al. 2020). Recently, some works devoted to using Neural ODEs combined with GNNs to characterise the continuous message-passing flow of node representations (Xhonneux et al. 2020; Poli et al. 2021). However, these methods are not built for dynamic graphs, nor can they tackle structural dynamics.

1.2. Paper organization and notations

The rest of this paper is structured as follows. In Section 2, we briefly introduce the background knowledge. In Section 3, we describe our main model, compare it with the competitors, and declare an approximation for efficient computation. The application in several representative graph representation learning tasks is also presented. In Section 4, we illustrate the empirical performance of our model in node attribute prediction task. Finally, we conclude in Section 5. The complete proofs will follow thereafter in the appendix.

Before continuing, we introduce several notations used throughout the paper. First of all, we use lower-case letters to denote scalars, bold lower-case letters to denote vectors, and bold upper-case letters to denote matrices. For a matrix \mathbf{X} , we represent the i -th row of \mathbf{X} as $\mathbf{X}^{(i)}$, and the element at the i -th row and j -th column as $\mathbf{X}^{(i,j)}$. We use \odot to represent element-wise (Hadamard) multiplication.

2. Preliminary

This section briefly reviews the basic definitions and common manners to learn graph embeddings, and then presents two typical neural differential equations.

2.1. Graph Embedding Learning

Static graph. A static graph only contains a fixed topological structure. Let a static graph represented as $\mathcal{G} = \{\mathcal{V}, \mathcal{E}\}$ where \mathcal{V} is the set of nodes, and $\mathcal{E} \subseteq \mathcal{V} \times \mathcal{V}$ is the set of edges. Let $v_i \in \mathcal{V}$ denote a node and $e_{ij} \in \mathcal{E}$ denote an edge between node v_i and v_j , $i, j \in \{1, \dots, |\mathcal{V}|\}$. Then the topology of the graph can be represented by an adjacency matrix $\mathbf{A} \in \mathbb{R}^{|\mathcal{V}| \times |\mathcal{V}|}$ where $\mathbf{A}^{(i,j)} = 1$ if $e_{ij} \in \mathcal{E}$ otherwise 0. In most complex scenarios, the graph is equipped with a node attribute matrix $\mathbf{F} = \{\mathbf{F}^{(i)}\}_{i=1}^{|\mathcal{V}|}$, $\mathbf{F}^{(i)} \in \mathbb{R}^m$ and edge feature matrix $\mathbf{E} = \{\mathbf{E}^{(i,j)}\}_{i,j=1}^{|\mathcal{V}|}$, $\mathbf{E}^{(i,j)} \in \mathbb{R}^w$. Graph embedding learning for static graphs is to create an embedding $\mathbf{z}(v_i)$ for each node v_i following a specified aggregation rule such that the specific local topology and node intrinsic information can be captured, formally

$$\mathbf{z}(v_i) = \sum_{j, \mathbf{A}^{(i,j)}=1} h(\text{msg}(\mathbf{F}^{(i)}, \mathbf{F}^{(j)}, \mathbf{E}^{(i,j)}), \mathbf{F}^{(i)}),$$

where msg and h are predefined or learnable functions.

Dynamic graphs. According to the interval of observations, dynamic graphs can be roughly categorized into *discrete-time dynamic graphs* and *continuous-time dynamic graphs* (Kazemi et al. 2020). A discrete-time dynamic graph comprises a chronological sequence of static graph snapshots regularly sampled according to a fixed time interval while a continuous-time dynamic graph consists of graph snapshots that are irregularly sampled. Dynamic graphs contain structural dynamics arising from edge addition or deletion, node addition or deletion events, and node intrinsic dynamics caused by node or edge feature transformations in different time stamps. As a result, the adjacency matrix \mathbf{A}_t can vary at different time stamps t . In this work, we embark on representation learning for continuous-time dynamic graphs where the observations are irregularly sampled. We start with undirected graphs (\mathbf{A}_t is symmetric) without time-varying node attributes and edge features, then we discuss the extensions to more subtle graph structures. It should be noted that our developed method can naturally deal with tasks on discrete-time dynamic graphs as well.

2.2. Neural Differential Equations

Neural ordinary differential equations (Neural ODEs). Neural ordinary differential equations (Chen et al. 2018) are the continuous-depth analogue to residual neural networks. Let $f_\theta : \mathbf{x} \rightarrow \mathbf{y}$ be a function mapping with some learnable parameters θ , and ζ_θ and ℓ_θ are two linear maps. Neural ODEs are defined as

$$\mathbf{z}_t = \mathbf{z}_0 + \int_0^t f_\theta(\mathbf{z}_s) ds \quad \text{and} \quad \mathbf{z}_0 = \zeta_\theta(\mathbf{x}), \quad (1)$$

here $\mathbf{y} \approx \ell_\theta(\mathbf{z}_T)$ can be utilized to approximate the desired output. In this formula, the solution \mathbf{z}_t is determined by the initial condition on \mathbf{z}_0 when θ has been learned. There exists no direct way to modify the trajectory given subsequent observations, let alone tackle structural dynamics in the data generation procedure, making the plain Neural ODEs not suitable for dynamic graph setups.

Neural controlled differential equations (Neural CDEs). Neural controlled differential equations (Kidger et al. 2020) are the continuous-time analogue to recurrent neural networks and provide a natural method for modeling temporal dynamics with neural networks.

Provide an irregularly sampled time series $\mathbf{x} = ((t_0, \mathbf{x}_{t_0}), (t_1, \mathbf{x}_{t_1}), \dots, (t_N, \mathbf{x}_{t_N}))$, with each $t_k \in \mathbb{R}$ the time stamp of the observation $\mathbf{x}_{t_k} \in \mathbb{R}^v$ and $t_0 < \dots < t_N$. Let $X : [t_0, t_N] \rightarrow \mathbb{R}^{v+1}$ be a continuous function of bounded variation with knots at t_0, \dots, t_N such that $X_{t_k} = (t_k, \mathbf{x}_{t_k})$. Let $f_\theta : \mathbb{R}^w \rightarrow \mathbb{R}^{w \times (v+1)}$ and $\zeta_\theta : \mathbb{R}^{v+1} \rightarrow \mathbb{R}^w$ are neural networks depending on their own learnable parameters θ . Then Neural CDEs can be defined as

$$\mathbf{z}_t = \mathbf{z}_{t_0} + \int_{t_0}^t f_\theta(\mathbf{z}_s) dX_s \quad \text{for } t \in (t_0, t_N], \quad (2)$$

where $\mathbf{z}_{t_0} = \zeta_\theta(t_0, \mathbf{x}_{t_0})$ and \mathbf{z}_t are the solution of the CDE. A key difference from Neural ODEs is the interpolation of observations to form a continuous path X_s , thus the dependency upon the time-varying data can be naturally incorporated into the integration process and the trajectory of the system can adapt according to the subsequent observations.

3. Main Results

In this section, we first present the embedding learning problem under evolving graphs. Then we introduce our proposed differential model. After that, we provide the applications to several representative graph-related tasks (e.g., node attributes prediction, dynamic node classification, temporal link prediction).

3.1. Problem Setup

Consider a dynamic graph generated following an underlying continuous procedure that we only observe a sequence of irregularly sampled graph snapshots $\mathcal{G} = \{(t_0, G_{t_0}), \dots, (t_N, G_{t_N})\}$, with each $t_k \in \mathbb{R}$ the time stamp of the observed graph G_{t_k} and $t_0 < \dots < t_N$. Among these observations, a graph snapshot $G_{t_k} = \{\mathcal{V}, \mathcal{E}\}$ is comprised of nodes $\mathcal{V} = \{v_1, \dots, v_{|\mathcal{V}|}\}$ and edges $\mathcal{E} \subseteq \mathcal{V} \times \mathcal{V}$ (we assume all snapshots share a common node set and edge set, and omit the subscript for simplicity). Commonly, we can represent the graph topological information for graph G_{t_k} via a time-specified adjacency matrix $\mathbf{A}_{t_k} \in \mathbb{R}^{|\mathcal{V}| \times |\mathcal{V}|}$ that each interaction $e_{ij} \in \mathcal{E}$ is valued in \mathbf{A}_{t_k} where $i, j \in \{1, \dots, |\mathcal{V}|\}$. Our goal is to learn a non-linear dynamical system on the dynamic graph \mathcal{G} based on the observations, formally the dynamics follow the form:

$$\mathbf{Z}_t = \mathbf{Z}_{t_0} + \int_{t_0}^t f(\mathbf{Z}_s) d\mathbf{X}_s \quad \text{for } t \in (t_0, t_N], \quad (3)$$

where $\mathbf{Z}_t = \{\mathbf{z}_t(v_i)\}_{i=1}^{|\mathcal{V}|}$, $\mathbf{Z}_t \in \mathbb{R}^{|\mathcal{V}| \times d}$ is output node embedding matrix, \mathbf{X} is an input signal path defined on $[t_0, t_N]$ which comprises the evolving topology of \mathcal{G} . The subscript notation here refers to function evaluation over time. When there exists an assigning function $\tau : \mathbb{R}^d \rightarrow \mathbb{R}^c$ on \mathcal{G} such that $\mathbf{Y}_t = \tau(\mathbf{Z}_t)$, $\mathbf{Y}_t \in \mathbb{R}^{|\mathcal{V}| \times c}$, this becomes by now an increasingly popular problem

with applications in several machine learning tasks such as node attribute prediction (Gao et al. 2016), dynamic node classification (Kumar et al. 2019), temporal link prediction (Nguyen et al. 2018) etc. Very recently, some works incorporate graph convolutional networks with ODEs for the continuous inference (Zang and Wang 2020; Yan et al. 2021; Choi et al. 2022), however, they degrade to an oversimplified setup where the neighborhood for nodes remains unchanged over time, making the proposed methods impractical for usage since the structural change could yield an unignorable effect on node embeddings. To make this problem solvable and the designed methods practical, we make the following assumption:

Assumption 1 (Continuity) *The evolving path $\mathbf{z} : [t_0, t_N] \rightarrow \mathbb{R}^d$ of each node embedding is absolutely continuous.*

This continuity assumption is standard for enabling differential equations (Chen et al. 2018; Kidger et al. 2020) and widely used by current dynamic graph approaches (Zang and Wang 2020; Wang et al. 2020; Yan et al. 2021; Choi et al. 2022).

3.2. GN-CDE: Graph Neural Controlled Differential Equations

Before introducing our differential equations, we need to prepare a continuously evolving path for graph structure first. Specifically, for a dynamic graph G_{t_k} collected at time stamp t_k endowed with adjacency matrix \mathbf{A}_{t_k} , we augment each interaction e_{ij} in \mathbf{A}_{t_k} by time stamp as $\hat{e}_{ij} = (t_k, e_{ij}) \in \mathbb{R}^2$ where $i, j \in \{1, \dots, |\mathcal{V}|\}$ such that all these processed interactions can be represented by a time augmented adjacency matrix as $\hat{\mathbf{A}}_{t_k} = (t_k, \mathbf{A}_{t_k}) \in \mathbb{R}^{|\mathcal{V}| \times |\mathcal{V}| \times 2}$. After that, we interpolate each possible interaction among two nodes independently utilizing the discrete observations to form a continuous path, this can be represented as $\hat{\mathbf{A}} : [t_0, t_N] \rightarrow \mathbb{R}^{|\mathcal{V}| \times |\mathcal{V}| \times 2}$ such that $\hat{\mathbf{A}}_{t_k} = (t_k, \mathbf{A}_{t_k})$. In this paper, we assume $\hat{\mathbf{A}}$ to be piecewise twice continuously differentiable with bounded second derivative, thus many interpolation schemes can be employed (Morrill et al. 2022).

Then, let $\zeta_\theta : \mathbb{R}^{|\mathcal{V}| \times |\mathcal{V}| \times 2} \rightarrow \mathbb{R}^{|\mathcal{V}| \times d}$ and $f_\theta : \mathbb{R}^{|\mathcal{V}| \times d} \times \mathbb{R}^{|\mathcal{V}| \times |\mathcal{V}|} \rightarrow \mathbb{R}^{|\mathcal{V}| \times d} \times \mathbb{R}^{|\mathcal{V}| \times |\mathcal{V}| \times 2}$ be two graph neural networks. We can define our controlled differential equation for dynamic graphs as

$$\mathbf{Z}_t = \mathbf{Z}_{t_0} + \int_{t_0}^t f_\theta(\mathbf{Z}_s, \mathbf{A}_s) d\hat{\mathbf{A}}_s \quad \text{for } t \in (t_0, t_N], \quad (4)$$

where $\mathbf{Z}_{t_0} = \zeta_\theta(t_0, \mathbf{A}_{t_0})$ is treated as the initial value to avoid translational invariance. One can utilize another linear function ℓ_θ to acquire the final prediction as $\tilde{\mathbf{Y}}_t = \ell_\theta(\mathbf{Z}_t)$, $\tilde{\mathbf{Y}}_t \in \mathbb{R}^{|\mathcal{V}| \times c}$. The notation “ $f_\theta(\mathbf{Z}_s, \mathbf{A}_s) d\hat{\mathbf{A}}_s$ ” in Eq. 4 represents a matrix-matrix product. Our formula differs from the standard Neural CDE presented in Kidger et al. (2020) in that we highlight the causal effect of graph structural dynamics via the defined path $\hat{\mathbf{A}}$, making it more suitable for the dynamic graphs scenarios, while Neural CDEs concentrate more on sequential relationships across observations rather than the graph structural dynamics. Based on this modification, \mathbf{A}_s in $f_\theta(\mathbf{Z}_s, \mathbf{A}_s)$ can strengthen such causal effect for the vector field update, and the derivative $d\hat{\mathbf{A}}_s$ can indicate the magnitudes and directions of the instantaneous change for the interactions.

Given f_θ implemented as a Graph Neural Network with the formula $f_\theta(\mathbf{Z}_s, \mathbf{A}_s) = \sigma(\mathbf{A}_s \mathbf{Z}_s^{(l)} \mathbf{W}^{(l)})$ where $\mathbf{W}^{(l)}$ is parameters for l -th layer GCN and σ is a rectified linear unit (ReLU) with a Lipschitz constant 1. In practice, we can leverage a regularized adjacency matrix of \mathbf{A}_s to stabilize the algorithm learning (Welling and Kipf 2016). Obviously, f_θ is global Lipschitz continuous, and we have the following theorem

Algorithm 1: Continuous inference of GN-CDE algorithm

Input: Sequentially observed topological structures of a dynamic graph $\{(t_0, \mathbf{A}_{t_0}), \dots, (t_N, \mathbf{A}_{t_N})\}$, initial function ζ_θ , vector field f_θ and decoder ℓ_θ

Initializing

- | $\hat{\mathbf{A}}$: Interpolate the time-augmented adjacency matrix
- | $\mathbf{Z}_{t_0} \leftarrow \zeta_\theta(t_0, \mathbf{A}_{t_0});$

end

Continuously inferring

- | $\mathbf{Z}_t \leftarrow \text{ODESolve}(\mathbf{Z}_{t_0}, \hat{\mathbf{A}}, t_0, t_N, f_\theta)$ following Eq. 5
- | $\tilde{\mathbf{Y}}_t \leftarrow \ell_\theta(\mathbf{Z}_t)$

end

return $\mathbf{Z}_t, \tilde{\mathbf{Y}}_t$

Theorem 2 *The solution \mathbf{Z}_t in Eq. 4 exhibits global existence and uniqueness.*

The proof is straightforward by using Picard–Lindelöf theorem (Coddington and Levinson 1955). We provide some theoretical comparisons of different interpolation schemes for our Graph Neural CDE model in Appendix C.

Evaluating. Provided $\hat{\mathbf{A}}$ as piecewise twice continuously differentiable with bounded second derivative, Eq. 4 can be rewritten as

$$\mathbf{Z}_t = \mathbf{Z}_{t_0} + \int_{t_0}^t f_\theta(\mathbf{Z}_s, \mathbf{A}_s) \frac{d\hat{\mathbf{A}}_s}{ds} ds \quad \text{for } t \in (t_0, t_N], \quad (5)$$

where $\mathbf{Z}_{t_0} = \zeta_\theta(t_0, \mathbf{A}_{t_0})$. This equation can be interpreted and solved as an ordinary differential equation, and one can solve our proposed GN-CDE model using the same technique for Neural ODEs (Kidger et al. 2020). Algorithm 1 depicts the continuous inference procedure of GN-CDE using an ODE solver.

3.3. Properties

Robustness to missing values. GN-CDE is capable of processing partially observed data. This is because each channel may independently be interpolated between observations to create $\hat{\mathbf{A}}_s$ in exactly the same manner as before.

Expressivity. Compared to representing the evolving graph structure via learnable parameters \mathbf{W} within GCN layers (Yan et al. 2018) or introducing additional neural network layers (Choi et al. 2022), our method can maintain the representation capability of GCN layers without introducing additional computational cost.

Calibration. Providing additional observations at intermediate time steps can help calibrate the inferred trajectory. This property is inherited from controlled differential equations (Kidger et al. 2020).

Memory-efficient. Our model can continuously incorporate incoming data without interrupting the differential equation, as a result, memory-efficient adjoint backpropagation may be performed for model training.

Discussion. The most similar work to this paper is STG-NCDE [Choi et al. \(2022\)](#) which employs Neural CDEs to learn the temporal and spatial dependencies for traffic forecasting tasks. Although this method is capable of tackling an unfixed graph structure via leveraging some learnable parameters to approximate the structure, it induces additional computational burden and cannot be extended to continuously evolving dynamic graphs. On the contrary, we define a generic framework that can incorporate the graph structural dynamics into the integration procedure naturally, thus no need to introduce additional parameters. Actually, STG-NCDE can be included in our framework presented for dynamic node classification task (See Section 3.6) by ignoring the dynamic structure and edge features.

3.4. Comparison to Alternative Models

In this section, we compare and discuss our framework with two alternatives that also combine dynamic graph structure with differential equations.

① Neural ODE

One choice for the alternative of Eq. 4 could be directly incorporating the graph structure into the vector field of Neural ODEs presented in Eq. 1 and define the graph neural ODE model as

$$\mathbf{Z}_t = \mathbf{Z}_{t_0} + \int_{t_0}^t f_\theta(\mathbf{Z}_s, \mathbf{A}_{\lfloor s \rfloor}) ds \quad \text{for } t \in (t_0, t_N], \quad (6)$$

where $\mathbf{Z}_{t_0} = \zeta_\theta(t_0, \mathbf{A}_{t_0})$, $\mathbf{A}_{\lfloor s \rfloor} = \mathbf{A}_{t_k}$ if $t_k \leq s < t_{i+1}$.

Theorem 3 *Any equation of the form $\mathbf{Z}_t = \mathbf{Z}_{t_0} + \int_{t_0}^t f_\theta(\mathbf{Z}_s, \mathbf{A}_{\lfloor s \rfloor}) ds$ may be represented exactly by a Graph Neural Controlled Differential Equation of the form $\mathbf{Z}_t = \mathbf{Z}_{t_0} + \int_{t_0}^t f_\theta(\mathbf{Z}_s, \mathbf{A}_s) d\hat{\mathbf{A}}_s$. However, the converse statement is not true.*

Proof The main proof idea is to build an intermediate differential model to bridge these two formulas. From Theorem 4 we know that, given a differential equation in the form $\mathbf{Z}_t = \mathbf{Z}_{t_0} + \int_{t_0}^t f_\theta(\mathbf{Z}_s) d\hat{\mathbf{A}}_s$, it can be represented by $\mathbf{Z}_t = \mathbf{Z}_{t_0} + \int_{t_0}^t f_\theta(\mathbf{Z}_s, \mathbf{A}_s) d\hat{\mathbf{A}}_s$. After that, we only need to proof any equation in the form $\mathbf{Z}_t = \mathbf{Z}_{t_0} + \int_{t_0}^t f_\theta(\mathbf{Z}_s, \mathbf{A}_{\lfloor s \rfloor}) ds$ can be represented by $\mathbf{Z}_t = \mathbf{Z}_{t_0} + \int_{t_0}^t f_\theta(\mathbf{Z}_s) d\hat{\mathbf{A}}_s$ which has been proofed by [Kidger et al. \(2020\)](#). See Appendix A.1 for more detailed proof. ■

According to Theorem 3, although the GN-ODE model can also take the dynamic graph structure into the vector field computational procedure, its representation ability is inferior to our proposed GN-CDE model.

② Neural CDE

Another alternative of Eq. 4 could be implementing the vector field without \mathbf{A}_s as input following the standard Neural CDEs presented in Eq. 2 which emphasizes the linear dependency on $d\hat{\mathbf{A}}_s$. We formulize this as

$$\mathbf{Z}_t = \mathbf{Z}_{t_0} + \int_{t_0}^t f_\theta(\mathbf{Z}_s) d\hat{\mathbf{A}}_s \quad \text{for } t \in (t_0, t_N], \quad (7)$$

where $\mathbf{Z}_{t_0} = \zeta_\theta(t_0, \mathbf{A}_{t_0})$.

Theorem 4 Any equation of the form $\mathbf{Z}_t = \mathbf{Z}_{t_0} + \int_{t_0}^t f_\theta(\mathbf{Z}_s) d\hat{\mathbf{A}}_s$ can be represented exactly by a Graph Neural Controlled Differential Equation of the form $\mathbf{Z}_t = \mathbf{Z}_{t_0} + \int_{t_0}^t f_\theta(\mathbf{Z}_s, \mathbf{A}_s) d\hat{\mathbf{A}}_s$ and vice versa.

Proof Here we sketch the proof idea. Since the vector field f_θ in $\mathbf{Z}_t = \mathbf{Z}_{t_0} + \int_{t_0}^t f_\theta(\mathbf{Z}_s, \mathbf{A}_s) d\hat{\mathbf{A}}_s$ takes both the \mathbf{Z}_s and \mathbf{A}_s as input, we can construct a stacked input $\beta_s = \begin{bmatrix} \mathbf{Z}_s \\ \mathbf{A}_s \end{bmatrix}$ for alternative such that the newly built controlled differential equation on β_s is equivalent to the Neural CDE formulation presented in Eq. 7. The full proof of Theorem 4 is detailed in Appendix A.2. ■

Although the dynamic graph can be learned by these two forms of CDE according to Theorem 4, they own different preferences during model learning stage. In the experimental part, we find that GN-CDE with non-linear dependency (as shown in Eq.4) performs better compared to the linear dependency variant (Eq.7). We conjecture that this is due to the fact that explicitly incorporating dynamic graph structure into the vector field allows for more precise control of information flow among nodes over time.

3.5. Approximation of GN-CDE

Directly implementing Eq. 5 by following Kidger et al. (2020) would result in an undesirable computational burden due to the high dimensional output of f_θ . For ease of computation and to ensure scalability to large neural networks, we consider some approximations to simplify this procedure via leveraging the message passing mechanism among graphs and the universal approximation property of graph neural networks. Given the naive graph as homogeneous and isotropic, the derivative on time stamp s can be shared by all interactions, and this enables the alternative between $d\hat{\mathbf{A}}_s$ and $d\mathbf{A}_s ds$ that the output dimension will be halved. Afterward, we fuse $d\mathbf{A}_s$ with \mathbf{A}_s in the vector field using a transformation matrix and produce a new adjacency matrix $\tilde{\mathbf{A}}_s$ that indicates the instantaneous structural change of graph, this yields two advantages: 1) the representations diffusion procedure by learnable parameters can be approximated via an adjusted graph structure; 2) the dimension of output for f_θ can be largely reduced, from $\mathbb{R}^{|\mathcal{V}| \times d} \times \mathbb{R}^{|\mathcal{V}| \times |\mathcal{V}| \times 2}$ to $\mathbb{R}^{|\mathcal{V}| \times d}$. Formularly, for a vector field parameterised by a L -layers graph neural network, the approximated equation that can be implemented much more efficiently as follows

$$\mathbf{Z}_t = \mathbf{Z}_{t_0} + \int_{t_0}^t \sigma(\tilde{\mathbf{A}}_s \mathbf{Z}_s^{(L)} \mathbf{W}^{(L)}) ds \quad \text{for } t \in (t_0, t_N], \quad (8)$$

where $\tilde{\mathbf{A}}_s = \begin{bmatrix} \mathbf{A}_s \\ \frac{d\mathbf{A}_s}{ds} \end{bmatrix} \mathbf{W}^{(DR)}$, $\mathbf{W}^{(DR)} \in \mathbb{R}^{2|\mathcal{V}| \times |\mathcal{V}|}$ is a transformation matrix for the fusion. Besides, $\mathbf{Z}_s^{(L)}$ can be acquired iteratively following the rule: $\mathbf{Z}_s^{(l)} = \sigma(\tilde{\mathbf{A}}_s \mathbf{Z}_s^{(l-1)} \mathbf{W}^{(l-1)})$ for $l \in \{1, \dots, L\}$, and σ is ReLU activation function.

Theorem 5 Eq. 8 is a valid approximation of our Graph Neural Controlled Differential Equation model with the form $\mathbf{Z}_t = \mathbf{Z}_{t_0} + \int_{t_0}^t f_\theta(\mathbf{Z}_s, \mathbf{A}_s) d\hat{\mathbf{A}}_s$.

Proof The full derivation of Theorem 5 is deferred to Appendix B, here we present several key steps. Consider our GN-CDE model presented in Eq. 5, it can be implemented using a L -layers graph

neural network directly as

$$\mathbf{Z}_t = \mathbf{Z}_{t_0} + \int_{t_0}^t \sigma(\mathbf{A}_s \mathbf{Z}_s^{(L)} \mathbf{W}^{(L)}) \mathbf{W}^{(\text{BR})} \frac{d\mathbf{A}_s}{ds} ds, \quad (9)$$

where $\mathbf{Z}_s^{(l)} = \sigma(\mathbf{A}_s \mathbf{Z}_s^{(l-1)} \mathbf{W}^{(l-1)})$ for $l \in \{1, \dots, L\}$. In Eq. 9, the parameter matrices $\mathbf{W}^{(L)}$ and $\mathbf{W}^{(\text{BR})}$ within $\sigma(\mathbf{A}_s \mathbf{Z}_s^{(L)} \mathbf{W}^{(L)}) \mathbf{W}^{(\text{BR})} \frac{d\mathbf{A}_s}{ds}$ can be combined and we obtain a new integrand $\sigma(\mathbf{A}_s \mathbf{Z}_s^{(L)} \mathbf{W}^{(\text{LBR})} \frac{d\mathbf{A}_s}{ds})$. After that, we introduce a transformation matrix $\mathbf{W}^{(\text{DR})}$ such that

$$\sigma\left(\begin{bmatrix} \mathbf{A}_s \\ \frac{d\mathbf{A}_s}{ds} \end{bmatrix} \mathbf{W}^{(\text{DR})} \mathbf{Z}_s^{(L)} \mathbf{W}^{(L)}\right) \approx \sigma(\mathbf{A}_s \mathbf{Z}_s^{(L)} \mathbf{W}^{(\text{LBR})} \frac{d\mathbf{A}_s}{ds}) \quad (10)$$

Finally, we utilize the universal approximation theorem (Scarselli et al. 2008) to verify that this approximation is valid. \blacksquare

Besides the theoretical analysis, we also provide an empirical comparison of this simplified version in Section 4 to assess its performance.

3.6. Applications

Node attributes prediction. For the node attributes prediction task, we are equipped with a node attributes matrix $\mathbf{F}_{t_k} \in \mathbb{R}^{|\mathcal{V}| \times m}$ containing m -dimensional attributes of the nodes for model training. When new edges and nodes emerge at time stamp t_k , \mathbf{A}_{t_k} and \mathbf{F}_{t_k} will evolve accordingly under the effects of graph structural dynamics and intrinsic dynamics of nodes. Our task is to predict the node attributes, *i.e.*, to predict \mathbf{F}_t at unseen time t based on the previous observations. To achieve this goal, we need to learn informative node representations $\mathbf{Z}_t \in \mathbb{R}^{|\mathcal{V}| \times d}$ that can be used for the prediction of the nodes attributes \mathbf{F}_t . The objective is to minimize the following expected loss

$$\min_{f_\theta, \ell_\theta} \mathbb{E}_t[\text{Loss}(\mathbf{F}_t, \tilde{\mathbf{Y}}_t)] \quad \text{for } t \in (t_0, T], \quad (11)$$

where $\tilde{\mathbf{Y}}_t = \ell_\theta(\mathbf{Z}_t)$ is the prediction based on \mathbf{Z}_t which is inferred by Eq. 4. We use the squared error to measure the mismatch between \mathbf{F}_t and $\tilde{\mathbf{Y}}_t$. Moreover, T can be $T \leq t_N$ which corresponds to interpolation prediction or $T > t_N$ corresponds to extrapolation prediction.

Dynamic node classification. The task of node classification is leveraging the collected information at time stamps $\{t_0, \dots, t_N\}$ to predict the label of nodes $\tilde{\mathbf{Y}}_t$ at time stamp $t, t > t_N$. The objective can be represented as

$$\min_{f_\theta, \ell_\theta} \mathbb{E}_t[\text{Loss}(\mathbf{Y}_t, \tilde{\mathbf{Y}}_t)] \quad \text{for } t \in (t_N, T], \quad (12)$$

where $\tilde{\mathbf{Y}}_t = \ell_\theta(\mathbf{Z}_t)$ is the prediction based on \mathbf{Z}_t and ℓ_θ is implemented as a MLP with a softmax activation function to obtain the class probability. We can use the squared loss or cross-entropy to measure the prediction error. Commonly, this works on attributed graphs, which means the node attribute matrix \mathbf{F}_{t_k} and edge feature matrix \mathbf{E} are provided in advance. Thus, the controlled differential equation can be written as

$$\mathbf{Z}_t = \mathbf{Z}_{t_0} + \int_{t_0}^t f_\theta(\mathbf{Z}_s, \mathbf{A}_s, \mathbf{F}_s, \mathbf{E}) d\hat{\mathbf{A}}_s \quad \text{for } t \in (t_0, t_N], \quad (13)$$

where $\mathbf{Z}_{t_0} = \zeta_\theta(t_0, \mathbf{A}_{t_0}, \mathbf{F}_{t_0}, \mathbf{E})$. In this equation, we need to interpolate the time augmented adjacency matrix as before and the node attribute matrix \mathbf{F}_{t_k} to conduct the integral. In addition, when \mathbf{F}_{t_k} or \mathbf{E} is not given, we can disable the corresponding terms in Eq. 13.

Temporal link prediction. This task is to predict the existence of an edge e_{ij} at time $t, t > t_N$. The node attribute matrix \mathbf{F}_{t_k} and edge feature matrix \mathbf{E} are also provided, thus we can follow the same setup designed for dynamic node classification tasks. To acquire the link probability among two nodes, we apply a MLP over the concatenation of the corresponding nodes’ embeddings.

4. Experimental Results

In this section, we conduct a comprehensive set of experiments on node attribute prediction tasks to validate the effectiveness of our proposed Graph Neural CDE model. More details of dataset construction and experimental setup can be found in the supplementary material.

Data. We consider two representative dynamic models: heat diffusion dynamics and gene regulatory dynamics. The underline networks own 400 nodes and are initialized as Grid network, Random network, Power-law network, Small world network, and Community network respectively, then some edges are randomly dropped or added occasionally to simulate the dynamic environments. After that, we irregularly sample 120 snapshots from the continuous-time dynamics to form the whole observations. The standard data splits presented in Zang and Wang (2020) are employed where 80 snapshots for training, 20 snapshots for testing the interpolation prediction task and 20 snapshots for testing the extrapolation prediction task.

Setup. The methods for comparison include Neural ODE (presented in Eq. 6) and Neural CDE (presented in Eq. 7). We use the natural cubic spline method as the interpolation scheme for all CDE-based methods since the interpolated path is smooth enough as twice differentiable (Kidger et al. 2020). Moreover, for a fair comparison, we keep the neural network architecture of the vector field part to be the same for all baselines for different benchmarks. We implement the vector field as one GCN layer with the dimension of output node embeddings $d = 20$. Then, all models are trained using Adam optimizer for 2,000 iterations, and the initial learning rate is set as 0.01. Finally, ℓ_1 loss is used as the evaluation metric. We report the results as the average value of 10 runs with the standard deviation shown aside.

Results. The test results of our method and competitive baselines throughout model optimization procedure for the node attribute prediction in heat diffusion and gene regulation dynamical systems are depicted in Fig. 1 and Fig. 2, respectively. We can observe that our GN-CDE model consistently outperforms other baselines, achieving a significantly lower test error across a variety of dynamic networks. In addition, compared to Neural ODE and Neural CDE, GN-CDE spends less time converging to stable results. These results demonstrate the capability and efficiency of our model in modeling the whole dynamics under evolving graph structures no matter for interpolation or for extrapolation tasks. It is worth noting that Neural ODE and Neural CDE exhibit comparable results in most scenarios, with the exception of heat diffusion prediction under grid and random structures, we conjecture the reason that Neural ODE primarily emphasizes on the structural dynamics in the vector field while Neural CDE primarily focuses on the dynamics in differential term, and only taking one aspect into account is insufficient for the representation learning on dynamic graphs.

In Fig. 3, we present a visualization of the ground truth dynamics and the learned dynamics by different methods in a heat diffusion dynamical system evolving with changing grid networks in order to gain insight into the the diverse learning behaviors of these methods. In the first panel of Fig. 3,

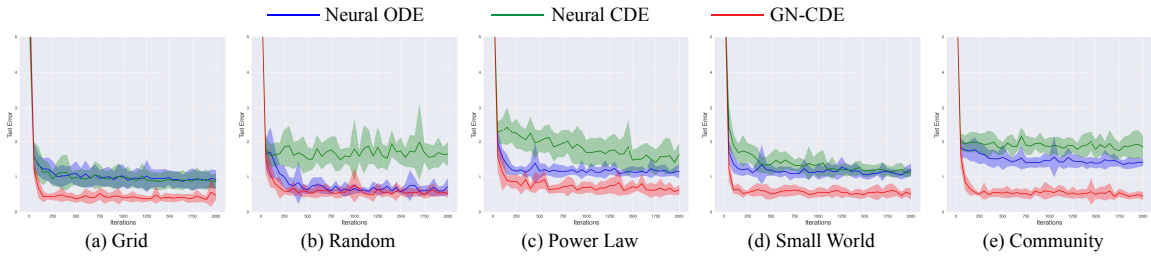


Figure 1: **Heat Diffusion:** The test errors of Neural ODE, Neural CDE and our GN-CDE models with respect to the optimization iteration count under five different graph structures: (a) grid, (b) Random, (c) power law, (d) small world and (e) community. We run each method 10 times and report the average ℓ_1 loss value with standard deviation. Here, the sum of extrapolation and interpolation results is presented for evaluating the performance among the whole dynamic procedure.

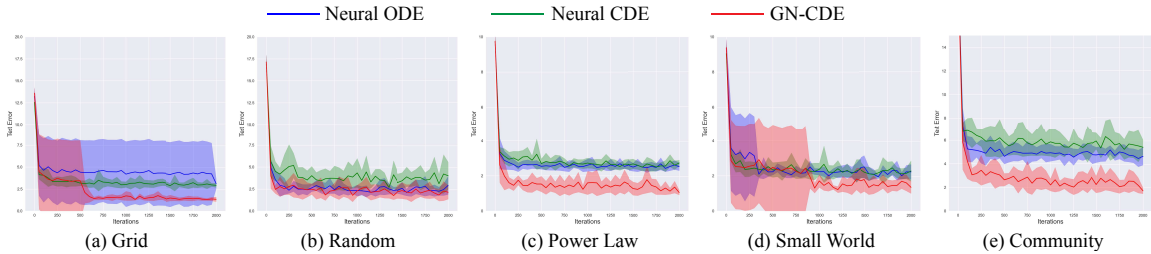


Figure 2: **Gene Regulation:** The test errors of Neural ODE, Neural CDE and our GN-CDE models with respect to the optimization iteration count under five different graph structures: (a) grid, (b) Random, (c) power law, (d) small world and (e) community. Here, the sum of extrapolation and interpolation ℓ_1 errors averaged over 10 runs is presented for performance evaluation.

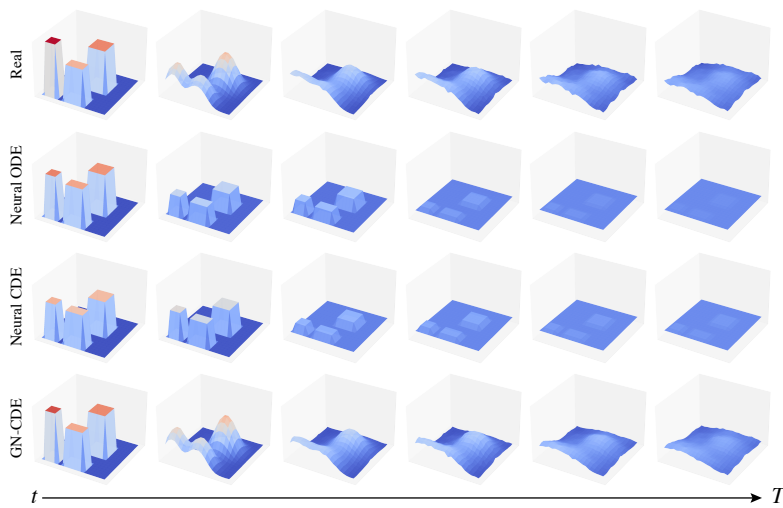


Figure 3: Visualisation of learned dynamics for heat diffusion over dynamic graphs. Our GN-CDE model fits the dynamics for the whole progress accurately.

we can observe several irregularities existing in the node attribute surface of the ground truth, which are attributed to the instantaneous structural changes during energy diffusion to neighboring nodes. However, both Neural ODE and Neural CDE fail to precisely fit the surface, let alone accurately capturing these structural changes. On the contrary, our GN-CDE model demonstrates excellent fitting of the dynamics across the entire time span.

5. Conclusion

In this paper, we propose a novel generic differential equations-based framework GN-CDE for representation learning on continuous-time dynamic graphs. GN-CDE creates graph paths into the controlled differential equation that the graph structural dynamics can be naturally incorporated when conduction integration. With this framework, we can apply it to solve different tasks on dynamic graphs with minor modifications. Experimental results on node attribute prediction tasks across different underlying graph structures demonstrate the superiority of our proposed method compared to other baselines.

References

- Amr Ahmed, Nino Shervashidze, Shravan Narayanamurthy, Vanja Josifovski, and Alexander J Smola. Distributed large-scale natural graph factorization. In *Proceedings of the 22nd international conference on World Wide Web*, pages 37–48, 2013.
- Mikhail Belkin and Partha Niyogi. Laplacian eigenmaps and spectral techniques for embedding and clustering. *Advances in neural information processing systems*, 14, 2001.
- Alaa Bessadok, Mohamed Ali Mahjoub, and Islem Rekik. Graph neural networks in network neuroscience. *IEEE Transactions on Pattern Analysis and Machine Intelligence*, 2022.
- Ricky TQ Chen, Yulia Rubanova, Jesse Bettencourt, and David K Duvenaud. Neural ordinary differential equations. *Advances in neural information processing systems*, 31, 2018.
- Xinshi Chen, Yan Zhu, Haowen Xu, Mengyang Liu, Liang Xiong, Muhan Zhang, and Le Song. Efficient dynamic graph representation learning at scale. *arXiv preprint arXiv:2112.07768*, 2021.
- Jeongwhan Choi, Hwangyong Choi, Jeehyun Hwang, and Noseong Park. Graph neural controlled differential equations for traffic forecasting. In *Proceedings of the AAAI Conference on Artificial Intelligence*, pages 6367–6374, 2022.
- Earl A Coddington and Norman Levinson. *Theory of Ordinary Differential Equations*. Tata McGrawHill Education, 1955.
- John R Dormand and Peter J Prince. A family of embedded runge-kutta formulae. *Journal of computational and applied mathematics*, 6(1):19–26, 1980.
- Wenqi Fan, Yao Ma, Qing Li, Yuan He, Eric Zhao, Jiliang Tang, and Dawei Yin. Graph neural networks for social recommendation. In *The world wide web conference*, pages 417–426, 2019.

- Pablo Gainza, Freyr Sverrisson, Federico Monti, Emanuele Rodola, D Boscaini, MM Bronstein, and BE Correia. Deciphering interaction fingerprints from protein molecular surfaces using geometric deep learning. *Nature Methods*, pages 184–192, 2020.
- Jianxi Gao, Baruch Barzel, and Albert-László Barabási. Universal resilience patterns in complex networks. *Nature*, 530(7590):307–312, 2016.
- Palash Goyal, Nitin Kamra, Xinran He, and Yan Liu. Dyngem: Deep embedding method for dynamic graphs. *arXiv preprint arXiv:1805.11273*, 2018.
- Will Hamilton, Zhitao Ying, and Jure Leskovec. Inductive representation learning on large graphs. *Advances in neural information processing systems*, 30, 2017.
- Seyed Mehran Kazemi, Rishab Goel, Kshitij Jain, Ivan Kobyzev, Akshay Sethi, Peter Forsyth, and Pascal Poupart. Representation learning for dynamic graphs: A survey. *J. Mach. Learn. Res.*, pages 1–73, 2020.
- Patrick Kidger, James Morrill, James Foster, and Terry Lyons. Neural controlled differential equations for irregular time series. *Advances in Neural Information Processing Systems*, pages 6696–6707, 2020.
- Srijan Kumar, Xikun Zhang, and Jure Leskovec. Predicting dynamic embedding trajectory in temporal interaction networks. In *Proceedings of the 25th ACM SIGKDD international conference on knowledge discovery & data mining*, pages 1269–1278, 2019.
- Shiyong Lan, Yitong Ma, Weikang Huang, Wenwu Wang, Hongyu Yang, and Pyang Li. Dstagnn: Dynamic spatial-temporal aware graph neural network for traffic flow forecasting. In *International Conference on Machine Learning*, pages 11906–11917, 2022.
- Yao Ma, Ziyi Guo, Zhaocun Ren, Jiliang Tang, and Dawei Yin. Streaming graph neural networks. In *Proceedings of the 43rd International ACM SIGIR Conference on Research and Development in Information Retrieval*, pages 719–728, 2020.
- Federico Monti, Karl Otness, and Michael M Bronstein. Motifnet: a motif-based graph convolutional network for directed graphs. In *2018 IEEE Data Science Workshop*, pages 225–228, 2018.
- James Morrill, Patrick Kidger, Lingyi Yang, and Terry Lyons. On the choice of interpolation scheme for neural CDEs. *Transactions of Machine Learning Research*, 2022.
- Giang Hoang Nguyen, John Boaz Lee, Ryan A Rossi, Nesreen K Ahmed, Eunye Koh, and Sungchul Kim. Continuous-time dynamic network embeddings. In *Companion proceedings of the the web conference 2018*, pages 969–976, 2018.
- Aldo Pareja, Giacomo Domeniconi, Jie Chen, Tengfei Ma, Toyotaro Suzumura, Hiroki Kanezashi, Tim Kaler, Tao Schardl, and Charles Leiserson. Evolvegn: Evolving graph convolutional networks for dynamic graphs. In *Proceedings of the AAAI Conference on Artificial Intelligence*, pages 5363–5370, 2020.
- Bryan Perozzi, Rami Al-Rfou, and Steven Skiena. Deepwalk: Online learning of social representations. In *Proceedings of the 20th ACM SIGKDD international conference on Knowledge discovery and data mining*, pages 701–710, 2014.

- Oswaldo L Podhajcer, Lorena Benedetti, Maria Romina Girotti, Federico Prada, Edgardo Salvatierra, and Andrea S Llera. The role of the matricellular protein sparc in the dynamic interaction between the tumor and the host. *Cancer and Metastasis Reviews*, pages 523–537, 2008.
- Michael Poli, Stefano Massaroli, Clayton M Rabideau, Junyoung Park, Atsushi Yamashita, Hajime Asama, and Jinkyoo Park. Continuous-depth neural models for dynamic graph prediction. *arXiv preprint arXiv:2106.11581*, 2021.
- Emanuele Rossi, Ben Chamberlain, Fabrizio Frasca, Davide Eynard, Federico Monti, and Michael Bronstein. Temporal graph networks for deep learning on dynamic graphs. *arXiv preprint arXiv:2006.10637*, 2020.
- Aravind Sankar, Yozen Liu, Jun Yu, and Neil Shah. Graph neural networks for friend ranking in large-scale social platforms. In *Proceedings of the Web Conference 2021*, pages 2535–2546, 2021.
- Stefania Sardellitti, Sergio Barbarossa, and Paolo Di Lorenzo. On the graph fourier transform for directed graphs. *IEEE Journal of Selected Topics in Signal Processing*, pages 796–811, 2017.
- Franco Scarselli, Marco Gori, Ah Chung Tsoi, Markus Hagenbuchner, and Gabriele Monfardini. Computational capabilities of graph neural networks. *IEEE Transactions on Neural Networks*, pages 81–102, 2008.
- Jian Tang, Meng Qu, Mingzhe Wang, Ming Zhang, Jun Yan, and Qiaozhu Mei. Line: Large-scale information network embedding. In *Proceedings of the 24th international conference on world wide web*, pages 1067–1077, 2015.
- Zekun Tong, Yuxuan Liang, Changsheng Sun, David S Rosenblum, and Andrew Lim. Directed graph convolutional network. *arXiv preprint arXiv:2004.13970*, 2020.
- Petar Veličković, Guillem Cucurull, Arantxa Casanova, Adriana Romero, Pietro Lio, and Yoshua Bengio. Graph attention networks. *arXiv preprint arXiv:1710.10903*, 2017.
- Junshan Wang, Guojie Song, Yi Wu, and Liang Wang. Streaming graph neural networks via continual learning. In *Proceedings of the 29th ACM international conference on information & knowledge management*, pages 1515–1524, 2020.
- Max Welling and Thomas N Kipf. Semi-supervised classification with graph convolutional networks. In *J. International Conference on Learning Representations*, 2016.
- Louis-Pascal Xhonneux, Meng Qu, and Jian Tang. Continuous graph neural networks. In *International Conference on Machine Learning*, pages 10432–10441, 2020.
- Da Xu, Chuanwei Ruan, Evren Korpeoglu, Sushant Kumar, and Kannan Achan. Inductive representation learning on temporal graphs. In *International Conference on Learning Representations*, 2020.
- Sijie Yan, Yuanjun Xiong, and Dahua Lin. Spatial temporal graph convolutional networks for skeleton-based action recognition. In *Thirty-second AAAI conference on artificial intelligence*, 2018.

Xu Yan, Xiaoliang Fan, Peizhen Yang, Zonghan Wu, Shirui Pan, Longbiao Chen, Yu Zang, and Cheng Wang. Contig: Continuous representation learning on temporal interaction graphs. *arXiv preprint arXiv:2110.06088*, 2021.

KChengxi Zang and Fei Wang. Neural dynamics on complex networks. In *Proceedings of the 26th ACM SIGKDD international conference on knowledge discovery & data mining*, pages 1269–1278, 2020.

Xitong Zhang, Yixuan He, Nathan Brugnone, Michael Perlmutter, and Matthew Hirn. Magnet: A neural network for directed graphs. *Advances in Neural Information Processing Systems*, pages 27003–27015, 2021.

Ling Zhong. A dynamic pandemic model evaluating reopening strategies amid covid-19. *PloS one*, page e0248302, 2021.

Jie Zhou, Ganqu Cui, Shengding Hu, Zhengyan Zhang, Cheng Yang, Zhiyuan Liu, Lifeng Wang, Changcheng Li, and Maosong Sun. Graph neural networks: A review of methods and applications. *AI Open*, 1:57–81, 2020.

Table of Contents

- [Appendix A:](#) Comparison to alternative CDE models
- [Appendix B:](#) Feasibility of Our Proposed GN-CDE Approximation
- [Appendix C:](#) Different Interpolation Schemes
- [Appendix D:](#) Other Types of Graph
- [Appendix E:](#) Further Empirical Results

Appendix A. Comparison to alternative CDE models

A.1. Proof of Theorem 3

From theorem 2, we know that any equation of the form $\mathbf{Z}_t = \mathbf{Z}_{t_0} + \int_{t_0}^t f_\theta(\mathbf{Z}_s) d\hat{\mathbf{A}}_s$ can be represented exactly by a GN-CDE of the form $\mathbf{Z}_t = \mathbf{Z}_{t_0} + \int_{t_0}^t f_\theta(\mathbf{Z}_s, \mathbf{A}_s) d\hat{\mathbf{A}}_s$, thus we can prove this theorem via showing that the equations of the form $\mathbf{Z}_t = \mathbf{Z}_{t_0} + \int_{t_0}^t f_\theta(\mathbf{Z}_s, \mathbf{A}_{[s]}) ds$ may be represented exactly by a GN-CDE of the form $\mathbf{Z}_t = \mathbf{Z}_{t_0} + \int_{t_0}^t f_\theta(\mathbf{Z}_s) d\hat{\mathbf{A}}_s$. This result follows directly from the Theorem 3.3 presented in [Kidger et al. \(2020\)](#) when unfolding the graph path $\hat{\mathbf{A}}_s$ for any time stamp s as a vector.

A.2. Proof of Theorem 4

Provide a dynamic graph comprising of a sequence of graph snapshots $\mathcal{G} = \{(t_0, G_{t_0}), \dots, (t_N, G_{t_N})\}$, with each $t_k \in \mathbb{R}$ the time stamp of the observed graph G_{t_k} and $t_0 < \dots < t_N$. Besides, each graph G_{t_k} is endowed with an adjacency matrix \mathbf{A}_{t_k} representing the topological information for G_{t_k} . Further, let $\hat{\mathbf{A}}_s$ be some continuous interpolation of \mathbf{A}_{t_k} such that $\hat{\mathbf{A}}_{t_k} = (t_k, \mathbf{A}_{t_k})$, then our GN-CDE model can be defined by

$$\mathbf{Z}_{t_0} = \zeta_\theta(t_0, \mathbf{A}_{t_0}), \quad \mathbf{Z}_t = \mathbf{Z}_{t_0} + \int_{t_0}^t f_\theta(\mathbf{Z}_s, \mathbf{A}_s) d\hat{\mathbf{A}}_s \quad \text{for } t \in (t_0, t_N]. \quad (14)$$

Let $\beta_s = \begin{bmatrix} \mathbf{Z}_s \\ \mathbf{A}_s \end{bmatrix}$, according to Eq. 14 we have

$$\beta_t = \begin{bmatrix} \mathbf{Z}_t \\ \mathbf{A}_t \end{bmatrix} = \begin{bmatrix} \mathbf{Z}_{t_0} \\ \mathbf{A}_{t_0} \end{bmatrix} + \int_{t_0}^t \begin{bmatrix} f_\theta(\mathbf{Z}_s, \mathbf{A}_s) \\ 1 \end{bmatrix} d\hat{\mathbf{A}}_s \quad \text{for } t \in (t_0, t_N]. \quad (15)$$

Then we can let $\tilde{f}_\theta(\beta_s) = \begin{bmatrix} f_\theta(\mathbf{Z}_s, \mathbf{A}_s) \\ 1 \end{bmatrix}$, the above equation can be rewrite as

$$\beta_t = \beta_{t_0} + \int_{t_0}^t \tilde{f}_\theta(\beta_s) d\hat{\mathbf{A}}_s \quad \text{for } t \in (t_0, t_N]. \quad (16)$$

This formulation is equivalent to the original Neural CDE formulation presented in [Kidger et al. \(2020\)](#), then we accomplish the proof.

Appendix B. Feasibility of Our Proposed GN-CDE Approximation

In this part, we show the detailed approximation steps of our implementation provided in Section 3.5. Considering the evaluation of GN-CDE model presented in Section 3.2 that

$$\mathbf{Z}_t = \mathbf{Z}_{t_0} + \int_{t_0}^t f_\theta(\mathbf{Z}_s, \mathbf{A}_s) \frac{d\hat{\mathbf{A}}_s}{ds} ds \quad \text{for } t \in (t_0, t_N]. \quad (17)$$

To enable the massaging passing of \mathbf{Z}_s over the graph structure, we can parameterize the vector field f_θ for \mathbf{Z}_t using a L -layers graph neural network followed by a fully-connected layer for projection purpose to compute the equation, that is

$$\mathbf{Z}_t = \mathbf{Z}_{t_0} + \int_{t_0}^t \sigma(\mathbf{A}_s \mathbf{Z}_s^{(L)} \mathbf{W}^{(L)}) \mathbf{W}^{(\text{BR})} \frac{d\mathbf{A}_s}{ds} ds, \quad (18)$$

where

$$\mathbf{Z}_s^{(l)} = \sigma(\mathbf{A}_s \mathbf{Z}_s^{(l-1)} \mathbf{W}^{(l-1)}) \quad \text{for } l \in \{1, \dots, L\}. \quad (19)$$

Considering the integrand $\sigma(\mathbf{A}_s \mathbf{Z}_s^{(L)} \mathbf{W}^{(L)}) \mathbf{W}^{(\text{BR})} \frac{d\mathbf{A}_s}{ds}$, rather than applying the final activation function before multiplying matrix-vector multiplying with $\mathbf{W}^{(\text{BR})} \frac{d\mathbf{A}_s}{ds}$, this can be applied afterward, so we can rewrite this term as

$$\sigma(\mathbf{A}_s \mathbf{Z}_s^{(L)} \mathbf{W}^{(L)} \mathbf{W}^{(\text{BR})} \frac{d\mathbf{A}_s}{ds}). \quad (20)$$

Since both $\mathbf{W}^{(L)}$ and $\mathbf{W}^{(\text{BR})}$ are learnable weights, we can replace them with a new learnable matrix $\mathbf{W}^{(\text{LBR})} \in \mathbb{R}^{d \times d \times |\mathcal{V}| \times |\mathcal{V}|}$, then we have

$$\sigma(\mathbf{A}_s \mathbf{Z}_s^{(L)} \mathbf{W}^{(\text{LBR})} \frac{d\mathbf{A}_s}{ds}). \quad (21)$$

In our implementation, we consider the following simplification to approximate the above formula

$$\sigma\left(\begin{bmatrix} \mathbf{A}_s \\ \frac{d\mathbf{A}_s}{ds} \end{bmatrix} \mathbf{W}^{(\text{DR})} \mathbf{Z}_s^{(L)} \mathbf{W}^{(L)}\right) \quad (22)$$

where $\mathbf{W}^{(\text{DR})} \in \mathbb{R}^{2|\mathcal{V}| \times |\mathcal{V}|}$ is a transformation matrix for the fusion between \mathbf{A}_s and $\frac{d\mathbf{A}_s}{ds}$. Besides, $\mathbf{Z}_s^{(L)}$ can be acquired iteratively by

$$\mathbf{Z}_s^{(l)} = \sigma\left(\begin{bmatrix} \mathbf{A}_s \\ \frac{d\mathbf{A}_s}{ds} \end{bmatrix} \mathbf{W}^{(\text{DR})} \mathbf{Z}_s^{(l-1)} \mathbf{W}^{(l-1)}\right) \quad \text{for } l \in \{1, \dots, L\}, \quad (23)$$

here, $\mathbf{W}^{(l)} \in \mathbb{R}^{|\mathcal{V}| \times |\mathcal{V}|}$. If we let $\tilde{\mathbf{A}}_s = \begin{bmatrix} \mathbf{A}_s \\ \frac{d\mathbf{A}_s}{ds} \end{bmatrix} \mathbf{W}^{(\text{DR})}$, then we can rewrite Eq. 22 and Eq. 23 as

$$\sigma\left(\tilde{\mathbf{A}}_s \mathbf{Z}_s^{(L)} \mathbf{W}^{(L)}\right) \quad (24)$$

where

$$\mathbf{Z}_s^{(l)} = \sigma\left(\tilde{\mathbf{A}}_s \mathbf{Z}_s^{(l-1)} \mathbf{W}^{(l-1)}\right) \quad \text{for } l \in \{1, \dots, L\}. \quad (25)$$

Now, we need to provide the following approximation for our implementation

$$\sigma\left(\tilde{\mathbf{A}}_s \mathbf{Z}_s^{(L)} \mathbf{W}^{(L)}\right) \approx \sigma(\mathbf{A}_s \mathbf{Z}_s^{(L)} \mathbf{W}^{(\text{LBR})} \frac{d\mathbf{A}_s}{ds}). \quad (26)$$

We verify this by considering the universal approximation property of graph neural networks.

Theorem 6 *Scarselli et al. (2008)*. Let \mathcal{D} be a graphical domain, for any measurable function $\tau \in \mathcal{F}(\mathcal{D})$, any norm $\|\cdot\|$ on \mathbb{R}^d , any probability measure P on \mathcal{D} and any reals ϵ, μ where $\epsilon > 0$ and $0 < \mu < 1$, there exist a GNN function φ that under mild assumptions can approximate τ perfectly, that is $P(\|\tau - \varphi\| \geq \epsilon) \leq 1 - \mu$.

For a graph G with the topological structure represented by \mathbf{A}_s , if we let $\varphi_1 = \sigma(\mathbf{A}_s \mathbf{Z}_s^{(L)} \mathbf{W}^{(LBR)} \frac{d\mathbf{A}_s}{ds})$, it can still approximate any function τ perfectly since the employed Sigmoid function $\sigma = \frac{1}{1+e^{-x}}$ keeps φ injective and continuous, and graph structure is well preserved. When we let $\varphi_2 = \sigma(\tilde{\mathbf{A}}_s \mathbf{Z}_s^{(L)} \mathbf{W}^{(L)})$, we then use the sparsity of graph structural changes, which means only very few elements in \mathbf{A}_s and $\frac{d\mathbf{A}_s}{ds}$ own values, and the combined adjacency matrix $\tilde{\mathbf{A}}_s$ will largely keep the original structure of \mathbf{A}_s , so φ_2 can approximate most functions of τ . As a result, we can make the approximate $\varphi_1 \approx \varphi_2$, that is $\sigma(\tilde{\mathbf{A}}_s \mathbf{Z}_s^{(L)} \mathbf{W}^{(L)}) \approx \sigma(\mathbf{A}_s \mathbf{Z}_s^{(L)} \mathbf{W}^{(LBR)} \frac{d\mathbf{A}_s}{ds})$.

Appendix C. Different Interpolation Schemes

Table 1: The comparison of different interpolation schemes.

Interpolation Schemes	Properties			
	Smoothness	Dependency on Future	Interpolation Complexity	Integral Difficulty
Linear	(piecewise)	One	Low	High
Rectilinear	(piecewise)	No	Lowest	High
Natural Cubic	✓	All	Highest	Lowest
Cubic Hermite	✓	One	High	Low

We consider four different interpolation schemes for our GN-CDE model: 1) Linear control; 2) Rectilinear control; 3) Natural cubic splines; 4) Cubic Hermite splines with backward differences. As we have analyzed the continuity of vector field $f_\theta(\mathbf{Z}_s, \mathbf{A}_s)$ and the existence and uniqueness of solutions for our framework in Section 3.2, in this part, we analyze the practical performance of them in the smoothness property, interpolation complexity and optimization difficulty when utilizing some ODE solvers (e.g., Euler method, Dormand-Prince (DOPRI) method (Dormand and Prince 1980)) for the integral. We summarize the results in Table 1.

Commonly, the ODE solvers calculate Eq. 5 use another form as

$$\frac{d\mathbf{Z}_t}{dt} = f_\theta(\mathbf{Z}_t, \mathbf{A}_t) \frac{d\hat{\mathbf{A}}t}{dt}. \quad (27)$$

We also utilize this formula to show different effects caused by the interpolation schemes for our GN-CDE model.

Linear control. If we have two observations (t_0, \mathbf{A}_{t_0}) and (t_2, \mathbf{A}_{t_2}) collected at time stamps t_0 and t_2 , respectively, and we want the get the value for time t_1 . Linear control is the interpolating along the straight line between these two observations. Formally, \mathbf{A}_{t_1} can be evaluated by solving the equation

$$\frac{\mathbf{A}_{t_1} - \mathbf{A}_{t_0}}{t_1 - t_0} = \frac{\mathbf{A}_{t_2} - \mathbf{A}_{t_1}}{t_2 - t_1}.$$

For our GN-ODE model, the vector field $f_\theta(\mathbf{Z}_t, \mathbf{A}_t)$ in Eq. 27 is implemented as GCN layers with the formula $f_\theta(\mathbf{Z}_s, \mathbf{A}_s) = \sigma(\mathbf{A}_s \mathbf{Z}_s^{(l)} W^{(l)})$, it is Lipschitz continuous. While for the derivation $\frac{d\hat{\mathbf{A}}_t}{dt}$, its value will be a constant when there exists a graph structural change otherwise zero. The multiplication of these two terms will exhibit some jumps due to the gradient discontinuities at the structural changing moment (t_k, \mathbf{A}_{t_k}) . Thus, this scheme owns moderate complexity for interpolation and high integral difficulty for the solvers to resolve the jumps.

Rectilinear control. For the observations $\{(t_0, \mathbf{A}_{t_0}), \dots, (t_N, \mathbf{A}_{t_N})\}$, rectilinear control updates the time and feature channels separately in lead-lag fashion as $\hat{\mathbf{A}}_t : [0, 2n] \rightarrow \mathbb{R}^{|\mathcal{V}| \times |\mathcal{V}| \times 2}$ such that $\hat{\mathbf{A}}_{2k} = (t_k, \mathbf{A}_{t_k})$ and $\hat{\mathbf{A}}_{2k+1} = (t_{k+1}, \mathbf{A}_{t_k})$.

When using rectilinear control as the interpolation scheme to build the path, the derivation $\frac{d\hat{\mathbf{A}}_t}{dt}$ for each possible interaction could appear with a large value when there exists a graph structural change. This leads to the derivation in Eq. 27 much more non-smooth than linear control. Besides, the length of the created path is twice as long as other schemes, thus it takes a longer time for our model to evaluate and train. The merit of this scheme is its low interpolation complexity since it only needs to pad the value for a time with the previous one.

Natural cubic splines. The natural cubic spline is a spline that uses the third-degree polynomial which satisfies the given control points. This is also the recommended scheme by Kidger et al. (2020).

With natural cubic splines, the created paths are twice differentiable. This means the ODE solvers do not need to resolve the jumps of $\frac{d\mathbf{Z}_t}{dt}$ since the derivation is smooth enough. Thus, the integral difficulty for this scheme is the lowest among the four discussed schemes. However, this scheme can lead to unacceptable time costs for path creation, especially when the scale of the graph is large.

Cubic Hermite splines with backward differences. For each interval $[t_k, t_{k+1})$ in among the whole observations $\{(t_0, \mathbf{A}_{t_0}), \dots, (t_N, \mathbf{A}_{t_N})\}$, cubic Hermite spline keeps that $\hat{\mathbf{A}}_{t_k} = (t_k, \mathbf{A}_{t_k})$ and $\hat{\mathbf{A}}_{t_{k+1}} = (t_{k+1}, \mathbf{A}_{t_{k+1}})$, and that the gradient at each node matches the backward finite difference as

$$\frac{d\hat{\mathbf{A}}_{t_k}}{dt} = \hat{\mathbf{A}}_{t_k} - \hat{\mathbf{A}}_{t_{k-1}} \quad \text{and} \quad \frac{d\hat{\mathbf{A}}_{t_{k+1}}}{dt} = \hat{\mathbf{A}}_{t_{k+1}} - \hat{\mathbf{A}}_{t_k}.$$

This scheme can smooth gradient discontinuities of linear control, thus its integration difficulty is lower than linear control. Besides, since it only needs to solve a single equation on each control point, its interpolation complexity is lower than natural cubic splines. However, the spurious delays in the spline will degrade the accuracy of our model.

See Ma et al. (2020) for more descriptions of these schemes.

Appendix D. Other Types of Graph

Our proposed GN-CDE model is not only a generic framework for tackling different graph-related tasks, such as the prediction of node attributes, dynamic nodes classification and temporal link prediction but can also be easily extended to more complex graph structures. We discuss how our model can be applied to solve tasks on directed graphs, multigraph, knowledge graphs, and heterogeneous information networks. An illustration of these graph structures is presented in Fig. 4.

Directed graph. Vertices in a directed graph are connected by directed edges (See Fig. 4(a)). In order to apply our GN-CDE model to tasks established upon directed dynamic graphs, it is necessary to modify our implementation of the vector field from graph convolutional layers defined for undirected

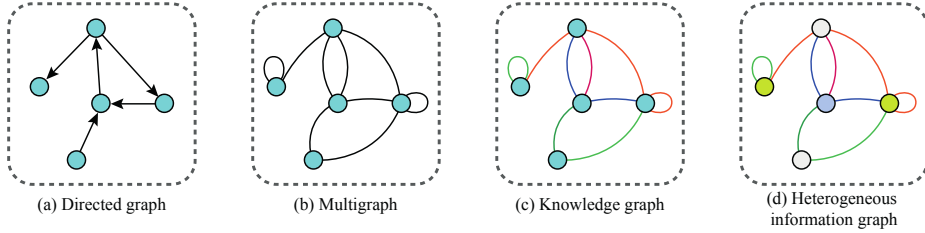


Figure 4: Illustration of other graph types.

graphs to directed graphs. In addition to utilizing an asymmetric adjacency matrix directly, we can also represent the graph structure with spectral-based methods that leverage edge direction proximity (Tong et al. 2020), transforms (Sardellitti et al. 2017; Zhang et al. 2021) or local graph motifs (Monti et al. 2018).

Multigraph. A graph in which there are multiple edges between two nodes (See Fig. 4(b)). The most common operations for performing graph convolution on a multigraph are graph fusion and separate subgraphs (Zhou et al. 2020). These techniques can cooperate with our GN-CDE model for representation learning on evolving multigraph.

Knowledge graph. This graph is a collection of real-world entities and the relational facts between pairs of entities. The underlining graph structure of the knowledge graph is commonly a multigraph with labeled edges, where the labels indicate the types of relationships (See Fig. 4(c)). In order to learn the graph embeddings, we would first utilize the graph fusion or separate subgraphs technique proposed for processing multigraph to acquire a single graph, then we employ the GN-CDE model presented in Eq. 13 but without node attributes matrix for the continuous inference, that is

$$\mathbf{Z}_t = \mathbf{Z}_{t_0} + \int_{t_0}^t f_{\theta}(\mathbf{Z}_s, \mathbf{A}_s, \mathbf{E}) d\hat{\mathbf{A}}_s \quad \text{for } t \in (t_0, t_N], \quad (28)$$

where $\mathbf{Z}_{t_0} = \zeta_{\theta}(t_0, \mathbf{A}_{t_0}, \mathbf{E})$.

Heterogeneous information networks. This is a complex graph type that consists of multiple types of nodes or edges (See Fig. 4(d)). In order to deal with the dynamic node types and edge features of heterogeneous information networks, we can directly apply the GN-CDE model presented in Eq. 13.

We recommend a comprehensive overview of graph neural networks (Zhou et al. 2020) for readers who are interested in exploring the extension of our GN-CDE model to various graph types.

Appendix E. Further Empirical Results

E.1. Data

Heat Diffusion Dynamics: The dynamics are governed by Newton’s law of cooling as follows,

$$\frac{d\mathbf{x}_t(v_i)}{dt} = -k^{(i,j)} \sum_{j=1}^n \mathbf{A}^{(i,j)} (\mathbf{x}(v_i) - \mathbf{x}(v_j)),$$

where $\mathbf{x}_t(v_i)$ represents the state of node v_i at time t and $\mathbf{A}^{(i,j)}$ is the heat capacity matrix represents the neighbors of each node v_i .

Table 2: Quantitative evaluation of prediction accuracy between GN-CDE and other baselines on node attribute prediction tasks. We run each method 10 times and report the average ℓ_1 loss value with standard deviation. Here, the sum of extrapolation and interpolation results is presented for evaluating the performance among the whole dynamic procedure. Best results are printed in boldface.

Model	Algorithms	Grid	Random	Power Law	Small World	Community
Heat Diffusion	Neural ODE	1.091 ± 0.344	0.629 ± 0.116	1.154 ± 0.189	1.093 ± 0.123	1.408 ± 0.091
	Neural CDE	0.962 ± 0.306	1.601 ± 0.471	1.642 ± 0.313	1.201 ± 0.179	1.857 ± 0.312
	GN-CDE	0.369 ± 0.134	0.521 ± 0.202	0.630 ± 0.135	0.484 ± 0.127	0.457 ± 0.112
Gene Regulation	Neural ODE	3.153 ± 0.562	3.732 ± 1.066	2.549 ± 0.226	2.252 ± 0.430	4.685 ± 0.759
	Neural CDE	2.967 ± 0.245	6.107 ± 3.202	2.764 ± 0.162	2.302 ± 0.591	5.325 ± 0.500
	GN-CDE	1.388 ± 0.262	2.193 ± 0.550	0.886 ± 0.072	1.331 ± 0.323	1.737 ± 0.260

Gene regulatory dynamics: The dynamics are governed by by Michaelis-Menten equation as follows,

$$\frac{d\mathbf{x}_t(v_i)}{dt} = -b_i\mathbf{x}(v_i)f + \sum_{j=1}^n \mathbf{A}^{(i,j)} \frac{\mathbf{x}^h(v_j)}{\mathbf{x}^h(v_j) + 1},$$

where the first term degradation when $f = 1$ or dimerization when $f = 2$.

E.2. Results

The digital evaluation results for Fig. 1 and Fig. 2 are presented in Table 2.